Bridging the Gap between Ionic Liquids and Molten Salts: Group 1 Metal Salts of the Bistriflamide Anion in the Gas Phase

ARTICLE *in* THE JOURNAL OF PHYSICAL CHEMISTRY B · APRIL 2009

Impact Factor: 3.3 · DOI: 10.1021/jp811039b · Source: PubMed

Bridging the Gap between Ionic Liquids and Molten Salts: Group 1 Metal Salts of the Bistriflamide Anion in the Gas Phase

João P. Leal,[†,‡] Manuel E. Minas da Piedade,*[,†] José N. Canongia Lopes,[§,∥] Alina A. Tomaszowska,[⊥] José M. S. S. Esperança,[§] Luís Paulo N. Rebelo,[§] and Kenneth R. Seddon[⊥]

Departamento de Química e Bioquímica, Faculdade de Ciências, Universidade de Lisboa, 1649-016 Lisboa, Portugal, Unidade de Ciências Químicas e Radiofarmacêuticas, Instituto Tecnológico e Nuclear, 2686-953 Sacavém, Portugal, Instituto de Tecnologia Química e Biológica, Universidade Nova de Lisboa, Av. República, Apartado 127, 2780-901 Oeiras, Portugal, Centro de Química Estrutural, Complexo Interdisciplinar, Instituto Superior Técnico da Universidade Técnica de Lisboa, 1049-001 Lisboa, Portugal, and The QUILL Centre, The Queen's University of Belfast, Stranmillis Road, Belfast BT9 5AG, U.K.

Received: December 15, 2008; Revised Manuscript Received: January 12, 2009

Fourier transform ion cyclotron resonance mass spectrometry experiments showed that liquid Group 1 metal salts of the bistriflamide anion undergoing reduced-pressure distillation exhibit a remarkable behavior that is in transition between that of the vapor−liquid equilibrium characteristics of aprotic ionic liquids and that of the Group 1 metal halides: the unperturbed vapors resemble those of aprotic ionic liquids, in the sense that they are essentially composed of discrete ion pairs. However, the formation of large aggregates through a succession of ion−molecule reactions is closer to what might be expected for Group 1 metal halides. Similar experiments were also carried out with bis{(trifluoromethyl)sulfonyl}amine to investigate the effect of H^+, which despite being the smallest Group 1 cation, is generally regarded as a nonmetal species. In this case, instead of the complex ion−molecule reaction pattern found for the vapors of Group 1 metal salts, an equilibrium similar to those observed for aprotic ionic liquids was observed.

Introduction

The idea that ionic liquids were essentially involatile was recently shown to be incorrect, when it was found that a variety of these substances could be distilled at low pressure without decomposition,[1] and the vapor pressures and enthalpies of vaporization of some ionic liquids were determined by Knudsen effusion,[2−4] transpiration,[5] mass spectrometry,[6] calorimetry,[7] or thermogravimetry.[8] This opened new perspectives in terms of exploring both novel synthetic routes and purification strategies, some of which with possible technological applications,[9,10] and also raised the fundamental question of elucidating the nature of the species present in the gaseous phase during the reduced-pressure distillation of ionic liquids.

In a previous publication, we investigated this problem using Fourier transform ion cyclotron resonance mass spectrometry (FT-ICR-MS).[11] The experiments demonstrated that the archetypal aprotic and thermally stable ionic liquids, 1-alkyl-3-methylimidazolium bis{(trifluoromethyl)sulfonyl}amide, $[C_n\text{mim}][NTf_2]$ ($n = 2$, 4, 6, 8, or 10; bis{(trifluoromethyl)sulfonyl}amide is commonly known as bistriflamide), 1-butyl-3-methylimidazolium hexafluorophosphate, $[C_4\text{mim}][PF_6]$, and trihexyltetradecylphosphonium trifluoromethyl sulfonate, $[P(C_{14}H_{29})(C_6H_{13})_3][OTf]$ (trifluoromethyl sulfonate is also known as triflate), distil under reduced pressure as neutral anion−cation pairs, without any detectable amounts of isolated ions or higher aggregates (charged or uncharged) in the vapor phase. This conclusion, which has also been supported by more recent studies,[12,13] corroborated the mass spectrometric results of Armstrong et al.[6] for the evaporation of thin films of ionic liquids into ultrahigh vacuum, and suggested that the detection of vapors containing isolated ions and higher aggregates in various other mass spectrometric experiments was due to the fact that these latter techniques are far from reproducing thermal distillation conditions.[14−23] Furthermore, the time evolution of the intensities of the FT-ICR-MS signals observed during the vaporization of the binary mixtures ($[C_4\text{mim}][NTf_2] + [C_4\text{mim}][PF_6]$) and ($[C_4\text{mim}][NTf_2] + [P(C_{14}H_{29})(C_6H_{13})_3][OTf]$) indicated the occurrence of fractional distillation.[11] Finally, the investigation of 1-methylimidazolium ethanoate, $[\text{Hmim}][O_2CCH_3]$,[11] gave experimental evidence that, as previously assumed,[1,24−26] the vaporization of this class of protic ionic liquids involves a proton transfer mechanism with formation of two volatile neutral molecules (in this case 1-methylimidazole and ethanoic acid) and, therefore, it is distinct from the vaporization of ionic liquids containing quaternized cations.

The picture that has developed from the study of the above-mentioned ionic liquid families is intrinsically different from that characteristic of Group 1 metal halides, MX (M = Li, Na, K, Rb, or Cs; X = F, Cl, Br, or I). These compounds melt well above room temperature (742−1269 K),[27−29] and the vapors originating from the liquids under low pressure show significant fractions of aggregates larger than ion pairs (particularly dimers).[27,30,31] The tendency for aggregation decreases as the sizes of the M^+ or X^- ions increase (e.g., LiCl > NaCl > KCl > RbCl > CsCl and NaF > NaCl > NaI).[30]

Historically, studies on molten salts and on ionic liquids have been performed under very different research regimens, and they are often regarded as different classes of materials. If these salts

* To whom correspondence should be addressed. E-mail: memp@fc.ul.pt.
† Universidade de Lisboa.
‡ Instituto Tecnológico e Nuclear.
§ Universidade Nova de Lisboa.
∥ Instituto Superior Técnico da Universidade Técnica de Lisboa.
⊥ The Queen's University of Belfast.

10.1021/jp811039b CCC: $40.75
Published on Web 02/24/2009

are considered to belong to different classes, then the materials investigated here are the missing link. Their properties lie in between, and there is a smooth transition from one extreme to the other. These are the salts composed of a Group 1 metal cation and a commonly used ionic liquid anion: $M(NTf_2)$ (M = Li, Na, K, Rb, Cs). Currently, these salts are under intensive investigation for lithium ion batteries and for the safety improvement (including reducing the operational heat released) of battery electrolytes in general. In particular, ionic liquid solutions of lithium bis{(trifluoromethyl)sulfonyl}amide, Li-(NTf_2), have been reported to possess excellent properties as electrolytes for lithium ion batteries.[32] Multiple-component melts of different $M(NTf_2)$ salts are expected to be even more useful than their single-salt counterparts for practical applications in electrochemical devices due to the conjugation of low melting temperatures with high lithium or sodium content.[33] It is our belief that understanding the thermal vaporization and the gas-phase behavior of these salts is highly valuable both from a fundamental perspective and a practical one as well. Therefore, in this work, we studied the thermal vaporization and the structure of the gas phase of all, from lithium to cesium, $M(NTf_2)$ salts. These compounds, and their mixtures, are solid at ambient temperature and pressure, but they melt[33−36] and subsequently distil at temperatures and pressures similar to those present in our previous investigation of $[C_n\text{mim}][NTf_2]$, $[C_4\text{mim}][PF_6]$, and $[P(C_{14}H_{29})(C_6H_{13})_3][OTf]$.[11]

Results and Discussion

The FT-ICR-MS experiments reported here have shown that when $M(NTf_2)$ molten salts distill at 600−680 K and 6×10^{-6} to 2×10^{-4} Pa, then, similarly to the previously studied aprotic ionic liquids, the vapor phase essentially consists of neutral ion pairs (in the case of conventional ionic liquids, only neutral ion pairs have been detected).[11] Contrasting with the behavior of aprotic ionic liquids, the ions formed by electron ionization (EI) exhibit a series of consecutive reactions with the neutral ion pairs to yield $[M_{n+1}(NTf_2)_n]^+$ or $[M_n(NTf_2)_{n+1}]^-$ aggregates of increasing molecular mass, where n is the number of neutral ion pairs. Moreover, in the case of $Li(NTf_2)$ and $Na(NTf_2)$, minor contributions from analogous reaction channels involving neutral aggregates higher than neutral ion pairs, $[M_n(NTf_2)_n]$ ($n > 1$), were observed.

Three other features, all in line with our previous experiments with conventional aprotic ionic liquids,[11] were noted. First, the major peaks in the FT-ICR mass spectra of the $M(NTf_2)$ vapors corresponded to the cationic, M^+, and anionic $(NTf_2)^-$ moieties present in the solid or liquid phase, and to fragment ions originating from NTf_2 (Figure 1). No peaks corresponding to parent radical ions $[M(NTf_2)]^{+\bullet}$ or $[M(NTf_2)]^{-\bullet}$ were detected, although recent mass spectrometric studies have shown that this might eventually be possible for the positive ions if field ionization (a softer ionization method) was available.[13]

Second, the absence of ionic species in the vapor phase of $M(NTf_2)$ was inferred from a series of experiments where positive and negative ion FT-ICR mass spectra were recorded as a function of the energy of the ionization beam, from 70 to 0 eV. As illustrated in Figure 2 for $Cs(NTf_2)$, the intensities of the Cs^+ (positive mode) and $(NTf_2)^-$ (negative mode) ions decrease as the energy of the electron beam decreases. No ions were detected when the electron-beam energy was set to zero.

Third, measurements at different temperatures showed a gradual increase of the intensities of the signals corresponding to the cation and anion as the temperature increased. This fact reflects the expected increase of the vapor pressure of the liquid with temperature.[3−6,11]

The most significant departure from the behavior of aprotic ionic liquids was the observation of a richer and more complex set of consecutive ion−molecule reactions, with patterns that vary with the nature of the Group 1 metal. This is illustrated in Figure 3, where the evolution of the positive ion spectra obtained for $Na(NTf_2)$ and $Cs(NTf_2)$ at different reaction times are compared.

The observed reactions primarily occurred through the sequences indicated in Schemes 1 (positive ions) and 2 (negative ions), where the M^+ or $(NTf_2)^-$ species generated by electron ionization (in positive or negative detection modes, respectively) initiate a process of consecutive reactions with the neutral ion pairs present in the vapor phase, to form progressively larger ionic aggregates. The largest $[M_{n+1}(NTf_2)_n]^+$ ions observed during a 10 s reaction time corresponded to $n = 10$ (M = Li), 9 (M = Na), 6−7 (M = K), 6 (M = Rb), and 5 (M = Cs). Aggregation leading to $[M_n(NTf_2)_{n+1}]^-$ clusters was also observed in the negative ion detection mode. However, for a given reaction time, the detected negative clusters were always smaller than their positive counterparts. In the case of sodium and cesium, for example, after a reaction time of 10 s, the largest $[M_n(NTf_2)_{n+1}]^-$ clusters found were $[Na_5(NTf_2)_6]^-$ and $[Cs(NTf_2)_2]^-$.

Contrasting with this behavior, no aggregates higher than $[A_2B]^+$ or $[AB_2]^-$ (A = cationic; B = anionic moiety) were found in our previous experiments with aprotic ionic liquids.[11] Only the first steps of the reaction sequences in Schemes 1 and 2 were observed, with the equilibrium between the species $[A_2X]^+$ or $[AX_2]^-$ and the corresponding precursors being attained without further consecutive or side reactions.

To investigate if the $[M_{n+1}(NTf_2)_n]^+$ and $[M_n(NTf_2)_{n+1}]^-$ clusters effectively resulted from consecutive reaction schemes and if neutral clusters of higher masses than neutral ion pairs were present in the vapor phase of $M(NTf_2)$, experiments such as that illustrated in Figure 4 for $Na(NTf_2)$ and $Cs(NTf_2)$ were carried out. In the latter case, the Cs^+ ion was first isolated and allowed to react with the neutral vapor according to Scheme 1. The spectrum obtained after a 2.5 s delay (Figure 4e) showed peaks at m/z = 133 (Cs^+), 546 ($[Cs_2(NTf_2)]^+$), and 959 ($[Cs_3(NTf_2)_2]^+$). A similar experiment was then performed with continuous ejection of the $[Cs_2(NTf_2)]^+$ ion. This led to the spectrum in Figure 4f, where the peaks at m/z = 546 and m/z = 959 are absent. This clearly indicates that $[Cs_2(NTf_2)]^+$ is the precursor of $[Cs_3(NTf_2)_2]^+$. The corresponding results for a delay time of 10 s and ejection of $[Cs_3(NTf_2)_2]^+$ are illustrated in Figure 4g and h. They show again that the ejection of a given cluster prevents the formation of all higher aggregates, thus proving that the positive ion−molecule reactions involving the cesium compound conform to Scheme 1. Analogous experiments showed that the corresponding negative ions reacted according to Scheme 2. Although an equivalent pattern was found for the potassium and rubidium salts, in the case of the lithium and sodium derivatives, a minor contribution from a reaction involving a $[M_2(NTf_2)_2]$ neutral aggregate was observed. This is clearly seen in Figure 4a−d, where the continuous ejection of a given aggregate does not completely eliminate the formation of larger aggregates through reactions such as

$$[M_n(NTf_2)_{n-1}]^+(g) + [M_2(NTf_2)_2](g) \rightarrow [M_{n+2}(NTf_2)_{n+1}]^+(g) \quad (1)$$

It can, therefore, be concluded that, under low pressure distillation conditions, the $M(NTf_2)$ compounds exhibit a

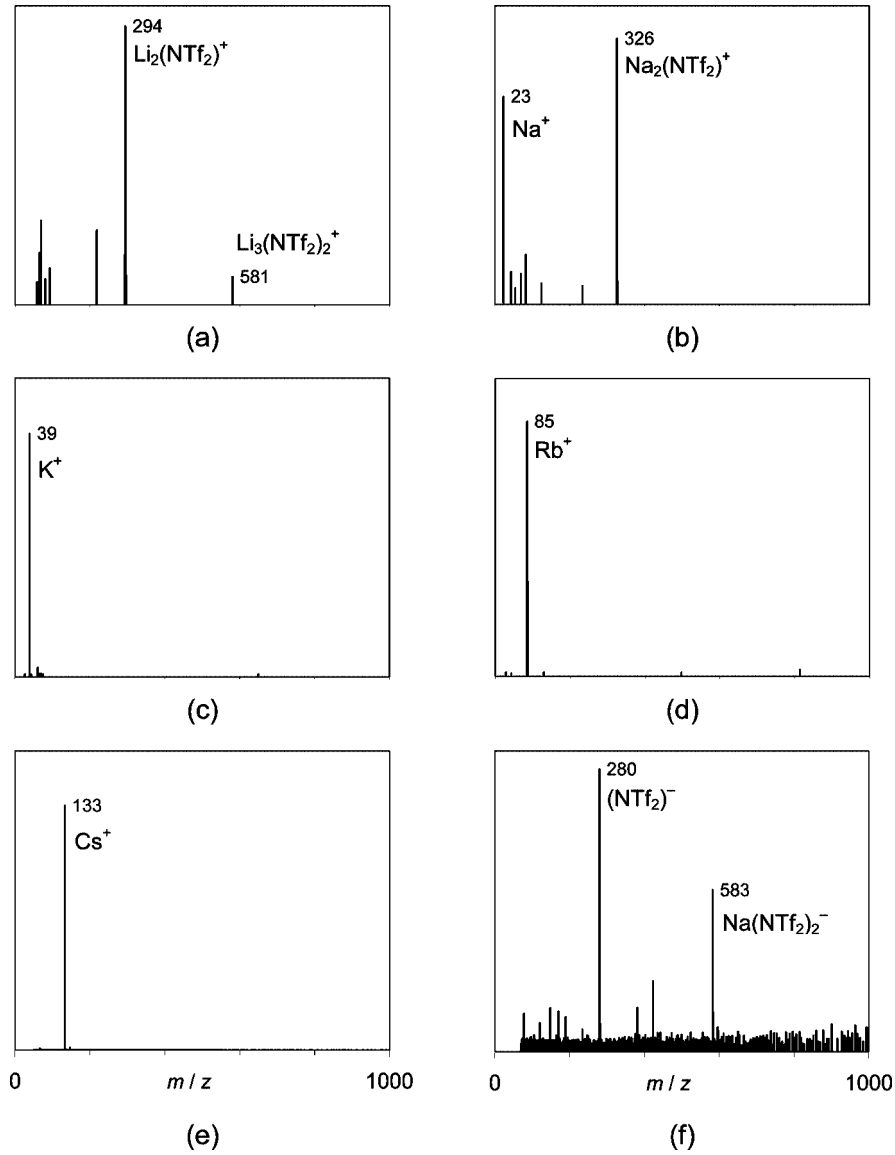

Figure 1. FT-ICR mass spectra of $Li(NTf_2)$, $Na(NTf_2)$, $K(NTf_2)$, $Rb(NTf_2)$, and $Cs(NTf_2)$, evaporating at 670 K. (a−e) Positive ion spectra. (f) Negative ion spectrum of $Na(NTf_2)$.

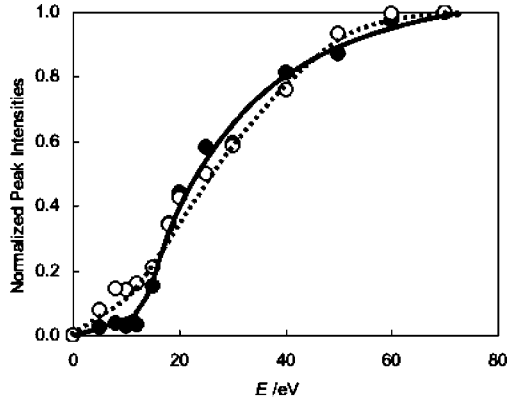

Figure 2. Ion intensities (given as fractions of the peak intensities at 70 eV) versus electron ionization energy for the cationic ($m/z = 133$, filled circles, continuous line) and anionic ($m/z = 280$, open circles, dotted line) moieties of $Cs(NTf_2)$ at 623 K and 6×10^{-6} Pa.

behavior somewhat intermediate between that of aprotic ionic liquids and that of Group 1 metal halides: they resemble aprotic ionic liquids, in the sense that the unperturbed vapor is essentially composed of discrete ion pairs $M(NTf_2)$. However, the observation of large $[M_{n+1}(NTf_2)_n]^+$ or $[M_n(NTf_2)_{n+1}]^-$ aggregates, generated through a sequence of ion−molecule reactions initiated by the M^+ and $(NTf_2)^-$ ions formed by electron ionization and the neutral species present in the vapor of the distilling $M(NTf_2)$ salt, is closer to what might be expected for Group 1 metal halides. Furthermore, the decreasing tendency for aggregation when the metal in $M(NTf_2)$ varies from Li to Cs also mimics that found for Group 1 metal halides.[30] This can be seen in Figure 5 where, for a given time, the reaction pattern leading to aggregation becomes less complex from Li to Cs. In the case of $Cs(NTf_2)$, the free cation and the smaller aggregates are prevalent, a situation which is closer to that observed for aprotic ionic liquids, as illustrated in Figure 6 for the previously studied $[C_6mim][NTf_2]$.[11]

The sequential character of the ion−molecule reactions leading to the ionic aggregates discussed above is also strikingly exemplified in Figure 7, which shows the FT-ICR mass spectrum of the vapor resulting from the distillation of a mixture of the five $M(NTf_2)$ (M = Li, Na, K, Rb, Cs) salts, acquired 1 s after electron ionization. Five regions, where different types of species predominate, can be distinguished in the figure: $m/z < 133$ (ionized metals), $294 < m/z < 546$ (blue; $[M_aM_b(NTf_2)]^+$), 581

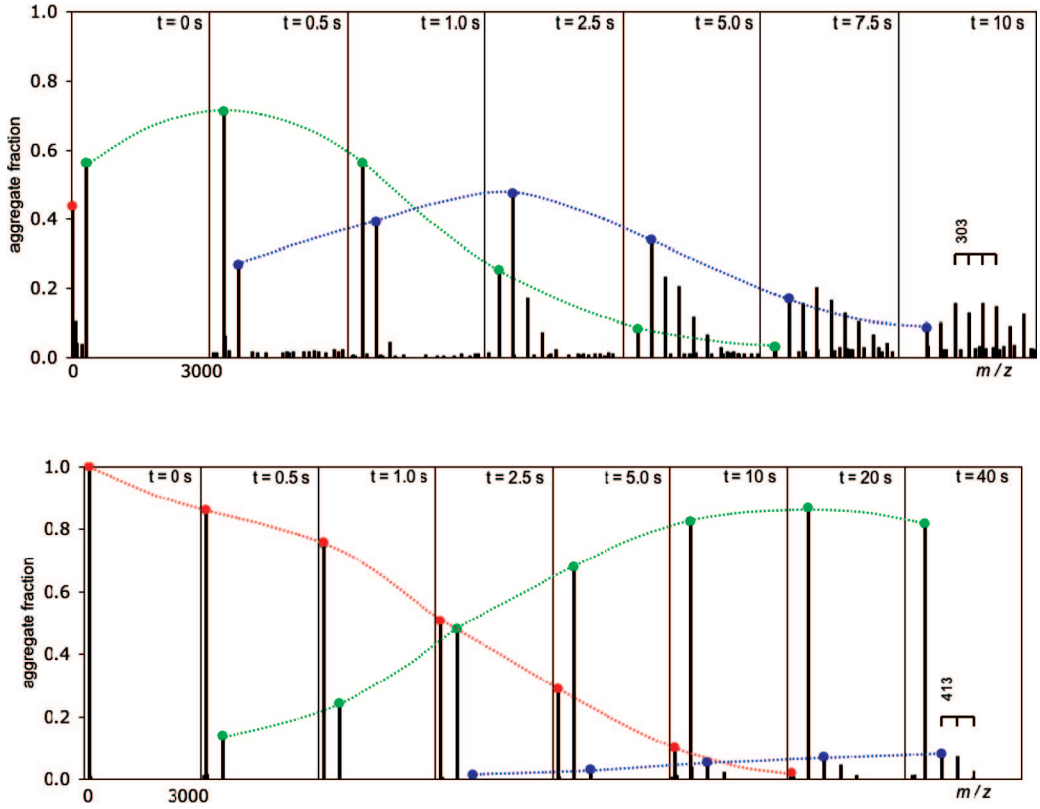

Figure 3. FT-ICR mass spectra of (top) $Na(NTf_2)$ and (bottom) $Cs(NTf_2)$ corresponding to different ion−molecule reaction times. The experiments were carried out at 663 K, with a nominal argon pressure in the vacuum chamber of 1.3×10^{-4} Pa. Selected peaks are labeled as follows: (top) red dot, $m/z = 23$ (Na^+); green dot, $m/z = 326$ ($[Na_2(NTf_2)]^+$); blue dot, $m/z = 629$ ($[Na_3(NTf_2)_2]^+$); (bottom) red dot, $m/z = 133$ (Cs^+); green dot, $m/z = 546$ ($[Cs_2(NTf_2)]^+$); blue dot, $m/z = 959$ ($[Cs_3(NTf_2)_2]^+$). The dotted lines are used just as guides to the eye (time does not increase regularly between spectra). The relevant peaks are spaced according to the mass of the corresponding neutral ion pairs: $m/z = 303$ for $Na(NTf_2)$ and $m/z = 413$ for $Cs(NTf_2)$.

SCHEME 1: Observed Cationic Reaction Sequences

$$M^+(g) + M(NTf_2)(g) \rightarrow [M_2(NTf_2)]^+(g)$$
$$[M_2(NTf_2)]^+(g) + M(NTf_2)(g) \rightarrow [M_3(NTf_2)_2]^+(g)$$
$$\cdots$$
$$[M_n(NTf_2)_{n-1}]^+(g) + M[NTf_2](g) \rightarrow [M_{n+1}(NTf_2)_n]^+(g)$$

SCHEME 2: Observed Anionic Reaction Sequences

$$(NTf_2)^-(g) + M(NTf_2)(g) \rightarrow [M(NTf_2)_2]^-(g)$$
$$[M(NTf_2)_2]^-(g) + M(NTf_2)(g) \rightarrow [M_2(NTf_2)_3]^-(g)$$
$$\cdots$$
$$[M_{n-1}(NTf_2)_n]^-(g) + M(NTf_2)(g) \rightarrow [M_n(NTf_2)_{n+1}]^-(g)$$

$< m/z < 959$ (red; $[M_aM_bM_c(NTf_2)_2]^+$), $868 < m/z < 1372$ (green; $[M_aM_bM_cM_d(NTf_2)_3]^+$), and $1155 < m/z < 1784$ (yellow; $[M_aM_bM_cM_dM_e(NTf_2)_4]^+$).

As expected, only Cs and Rb ions were detected for $m/z < 133$, because lighter Group 1 metals have already reacted after 1 s (see, for example, the case of $Na(NTf_2)$ in Figure 3). In the two next regions, almost all of the 15 possible Group 1 metal combinations for $[M_aM_b(NTf_2)]^+$ and 35 for $[M_aM_bM_c(NTf_2)_2]^+$ were found. The exceptions refer to $[LiM(NTf_2)]^+$ species, which were probably not observed due to the existence of faster ion−molecule reaction channels for Li^+ and its aggregates. In the case of $[M_aM_bM_c(NTf_2)_2]^+$, the most intense peaks do not correspond to ions containing Cs^+ or Rb^+. This is consistent with the aforementioned decreasing tendency for aggregation when the metal varies from Li to Cs. Interestingly, a very small peak at $m/z \sim 1408$ was found, which could be assigned to $[LiNaKRbCs(NTf_2)_4]^+$, an aggregate containing all studied Group 1 metals.

Finally, experiments with bis{(trifluoromethyl)sulfonyl}amine, $HNTf_2$, were carried out to investigate the effect of the simplest possible cation, H^+. This compound has a melting point of ~327 K and a very low normal boiling point (~383 K) as compared to the $M(NTf_2)$ salts.[34,35] It was therefore allowed to sublime at room temperature into the chamber of the FT-ICR mass spectrometer. The pressure conditions inside the chamber, before and after thermalization, were, however, set to approximately match those used in the $M(NTf_2)$ experiments. Since it was not possible to observe H^+ (the lower detection limit of the spectrometer is $m/z \sim 14$), only the $[H_2(NTf_2)]^+$ ionic aggregate was detected, isolated, and allowed to react. The fact that no additional species were found in those reactions indicates that the sequence in Scheme 1 does not occur in the case of $HNTf_2$. Concerning the negative ions, when $(NTf_2)^-$ was isolated and allowed to react with the neutral species present in the vapor, only $[H(NTf_2)_2]^-$ was observed, even with the detection set for delays longer than 10 s. Further kinetic studies indicated that, analogously to our previous findings for aprotic ionic liquids,[11] an equilibrium corresponding to the first step of Scheme 2

$$(NTf_2)^-(g) + M(NTf_2)(g) \rightleftharpoons [M(NTf_2)_2]^-(g) \qquad (2)$$

was attained. This is illustrated in Figure 8, which shows the kinetic profiles obtained for the $HNTf_2$ system when reaction 2 was approached from both sides. The forward process was studied by isolating the $(NTf_2)^-$ ion, allowing it to react with the neutral vapor, and setting the detection at increasing delay times (Figure 8a). Then, the $[H(NTf_2)_2]^-$ aggregate was isolated and the reverse reaction was investigated by a similar procedure, leading to the results in Figure 8b. It can be concluded from

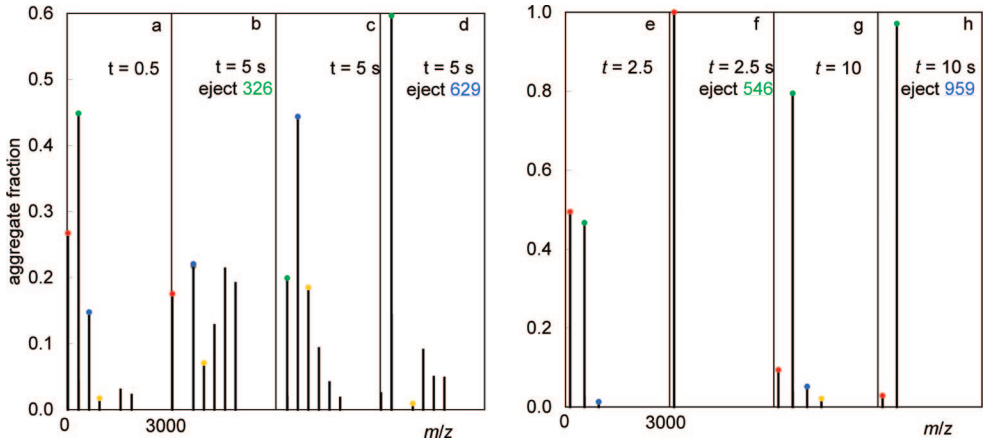

Figure 4. FT-ICR mass spectra of (left) $Na(NTf_2)$ and (right) $Cs(NTf_2)$, corresponding to different ion−molecule reaction times, with and without the ejection of selected ionic aggregates. For $Na(NTf_2)$, the experiments were carried out at $T = 643$ K, with a nominal argon pressure in the vacuum chamber of $p = 1.0 \times 10^{-4}$ Pa. The peaks are labeled as follows: red dot, $m/z = 23$ (Na^+); green dot, $m/z = 326$ ($[Na_2(NTf_2)]^+$); blue dot, $m/z = 629$ ($[Na_3(NTf_2)_2]^+$); yellow dot, $m/z = 932$ ($[Na_4(NTf_2)_3]^+$). In the case of $Cs(NTf_2)$, $T = 663$ K and $p = 1.3 \times 10^{-4}$ Pa. The peaks are labeled as follows: red dot, $m/z = 133$ (Cs^+); green dot, $m/z = 546$ ($[Cs_2(NTf_2)]^+$); blue dot, $m/z = 959$ ($[Cs_3(NTf_2)_2]^+$); yellow dot, $m/z = 1371$ ($[Cs_4(NTf_2)_3]^+$).

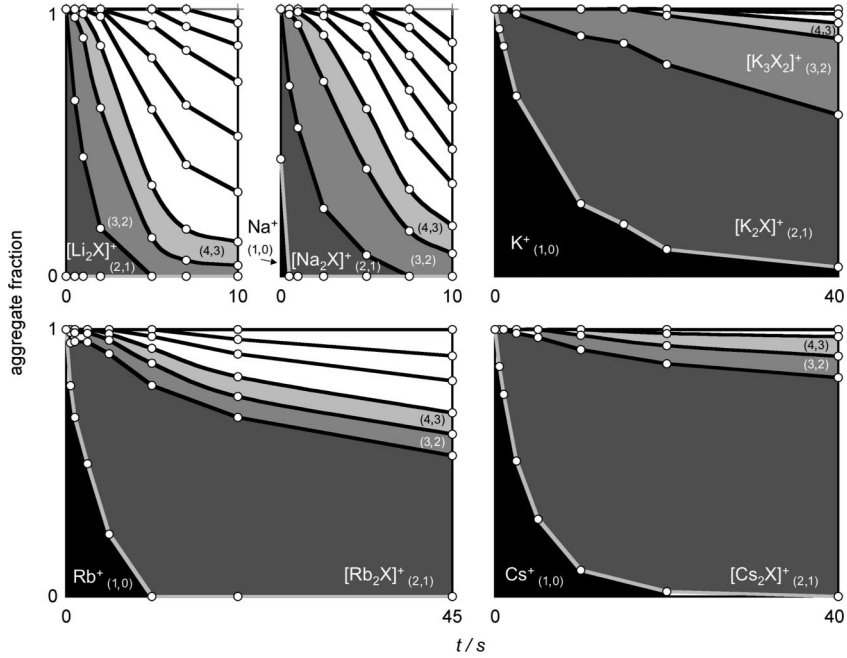

Figure 5. Aggregate distribution as a function of ion−molecule reaction time for the five Group 1 metal bistriflamide salts studied in this work. The reactions were carried out in positive detection mode at ~660 K, with nominal pressures in the vacuum chamber of $\sim 1 \times 10^{-4}$ Pa. The areas in black correspond to the free Group 1 cation species (Li^+ is not detectable in these experiments, since its mass is smaller than the lower m/z limit of the spectrometer), whereas the gradually lighter gray areas correspond to progressively larger aggregates. The numbers in parentheses denote the number of cationic and anionic species in each cluster. Aggregates larger than (4, 3) are not labeled in the graphs, but their presence can be inferred from the lines separating the white areas.

Figure 8 that the same equilibrium position is approximately reached from the direct and reverse directions.

Clearly, the behavior of the $HNTf_2$ vapor differs from that of the gaseous $M(NTf_2)$ compounds. At least in the negative ion detection mode, instead of a complex reaction pattern such as that in Scheme 2, an equilibrium similar to those observed for aprotic ionic liquids (reaction 2) is reached.

Experimental Section

General. Elemental analysis (C, H, N) was carried out on a Perkin-Elmer P2400 CHNS elemental analyzer. The method was UKAS accredited (certificate number 2033). Differential scanning calorimetry (DSC) experiments were made on a Perkin-Elmer DSC 7 apparatus. The samples, with masses in the range

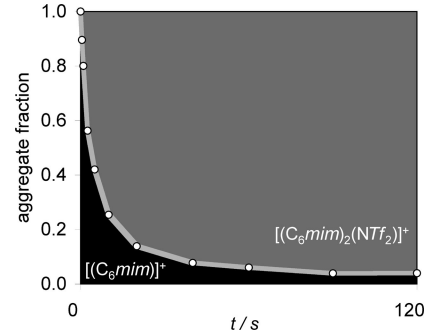

Figure 6. Aggregate distribution as a function of the ion−molecule reaction time for 1-hexyl-3-methylimidazolium bistriflamide, $[C_6mim][NTf_2]$ (see text).

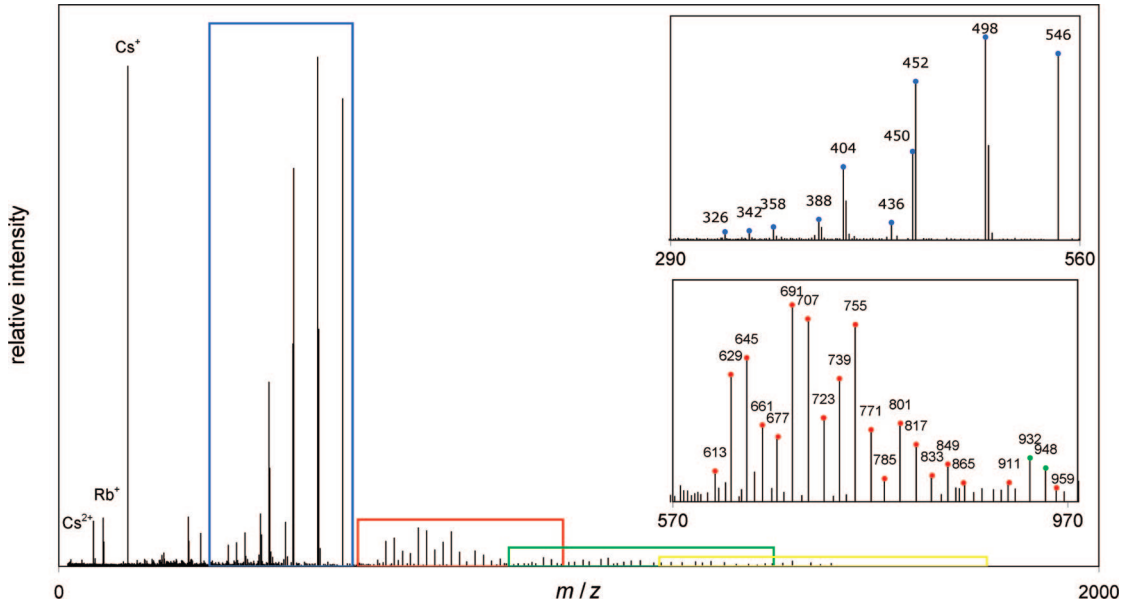

Figure 7. Positive mode FT-ICR mass spectrum of the vapor from a liquid mixture containing all five $M(NTf_2)$ salts studied in this work (M = Li, Na, K, Rb, and Cs). The experiment was carried out at 623 K, with a nominal argon pressure in the vacuum chamber of 1.3×10^{-4} Pa and a delay time of 1 s. The four colored rectangles indicate the ranges where different types of ionic aggregates can be found: $[M_aM_b(NTf_2)]^+$ in blue, $[M_aM_bM_c(NTf_2)_2]^+$ in red, $[M_aM_bM_cM_d(NTf_2)_3]^+$ in green, and $[M_aM_bM_cM_dM_e(NTf_2)_4]^+$ in yellow. The two insets show peak assignments (in the first two regions). Blue dots: 326 = $[Na_2(NTf_2)]^+$; 342 = $[NaK(NTf_2)]^+$; 358 = $[K_2(NTf_2)]^+$; 388 = $[NaRb(NTf_2)]^+$; 404 = $[KRb(NTf_2)]^+$; 436 = $[NaCs(NTf_2)]^+$; 450 = $[Rb_2(NTf_2)]^+$; 452 = $[KCs(NTf_2)]^+$; 498 = $[RbCs(NTf_2)]^+$; 546 = $[Cs(NTf_2)]^+$. Red dots: 613 = $[Li_2K(NTf_2)_2]^+$ and $[LiNa_2(NTf_2)_2]^+$; 629 = $[LiNaK(NTf_2)_2]^+$ and $[Na_3(NTf_2)_2]^+$; 645 = $[LiK_2(NTf_2)_2]^+$ and $[Na_2K(NTf_2)_2]^+$; 661 = $[NaK_2(NTf_2)_2]^+$; 677 = $[K_3(NTf_2)_2]^+$; 691 = $[LiKRb(NTf_2)_2]^+$ and $[Na_2Rb(NTf_2)_2]^+$; 707 = $[NaKRb(NTf_2)_2]^+$; 723 = $[LiNaCs(NTf_2)_2]^+$ and $[K_2Rb(NTf_2)_2]^+$; 739 = $[LiKCs(NTf_2)_2]^+$ and $[Na_2Cs(NTf_2)_2]^+$; 755 = $[NaKCs(NTf_2)_2]^+$; 771 = $[K_2Cs(NTf_2)_2]^+$; 785 = $[LiRbCs(NTf_2)_2]^+$; 801 = $[NaRbCs(NTf_2)_2]^+$; 817 = $[KRbCs(NTf_2)_2]^+$; 833 = $[LiCs_2(NTf_2)_2]^+$; 849 = $[NaCs_2(NTf_2)_2]^+$; 865 = $[KCs_2(NTf_2)_2]^+$; 911 = $[RbCs_2(NTf_2)_2]^+$; 959 = $[Cs_3(NTf_2)_2]^+$. Green dots: 932 = $[Li_2K_2(NTf_2)_3]^+$, $[LiNa_2K(NTf_2)_3]^+$, and $[Na_4(NTf_2)_3]^+$; 948 = $[Na_3K(NTf_2)_3]^+$ and $[LiNaK_2(NTf_2)_3]^+$.

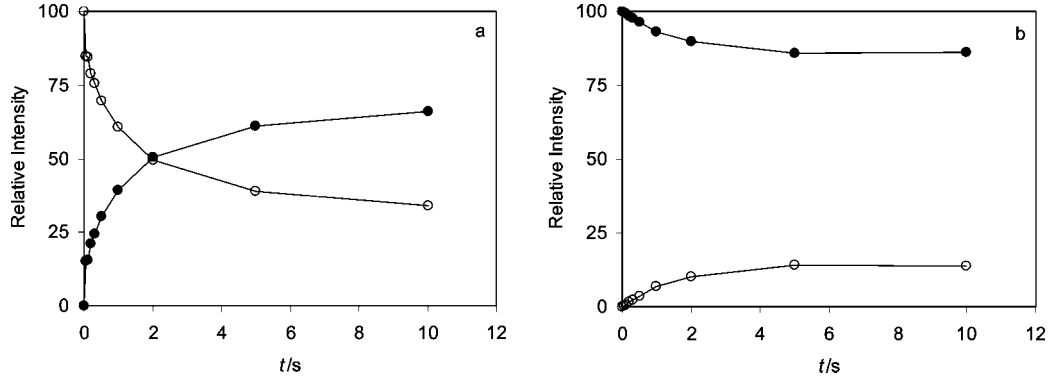

Figure 8. Kinetic profiles of the forward (a) and reverse (b) reaction 2. The open circles refer to $[NTf_2]^-$ (m/z = 280) and the filled circles to $[H(NTf_2)_2]^-$ (m/z = 561). The data were normalized so that the sum of the relative intensities of the peaks corresponding to the reactant and product ions is 100%.

of 5.0−10.0 mg, were sealed under nitrogen in aluminum pans, and weighed to $\pm 10^{-4}$ g on a Sartorius balance. Nitrogen (BOC) at a flow rate of 20 $cm^3 \cdot min^{-1}$ was used as the purging gas. The scan rate was β = 10 $K \cdot min^{-1}$. Thermogravimetric (TG) analyses were performed in the range 323−813 K, on a Perkin-Elmer Pyris ITGA, using platinum crucibles. The samples had masses in the range of 5.0−10.0 mg. Nitrogen (BOC) at a flow rate of 20 $cm^3 \cdot min^{-1}$ was used as the purging gas. The scan rate was β = 5 $K \cdot min^{-1}$.

Materials. The samples of bis{(trifluoromethyl)sulfonyl}amine, $HNTf_2$ (Aldrich, CAS 82113-65-3, 95%), and lithium bis{(trifluoromethyl)sulfonyl}amide, $Li(NTf_2)$ (3M, HQ-115, 98-100%), used in the FT-ICR-MS experiments were not further purified. All other $M(NTf_2)$ (M = Na, K, Rb, and Cs) compounds were synthesized from the reaction of $HNTf_2$, with the appropriate M_2CO_3 salt. The $HNTf_2$ used for synthetic purposes was first prepared by dissolving 15 g of $Li(NTf_2)$ in 15 g of concentrated H_2SO_4 (Aldrich, 95.0−98.0%) inside a round-bottom flask that was part of a Kugelrohr apparatus. The mixture was distilled in a vacuum (6 Pa) at 333 K (above the temperature of fusion of $HNTf_2$, T_{fus} = 325−329 K)[34,37] to yield pure $HNTf_2$ in the form of white crystals. Typically, 10 g of the solidified $HNTf_2$ distillate was mixed with the M_2CO_3 salt in a ca. 2.5:1.0 molar ratio. The mixture was heated to 403 K, and left under magnetic stirring until all of the carbonate had dissolved in the melted $HNTf_2$ and the evolution of CO_2 ceased (around 0.5 h). The reaction mixture was transferred to a Kugelrohr apparatus and the excess $HNTf_2$ removed by distillation at 6 Pa and 333 K. The solid residue was dissolved in methanol and the resulting solution filtered. The filtrate was taken to dryness in a rotary evaporator, to yield the $M(NTf_2)$ salt. The residual solvent was removed by distillation at 6 Pa and 423 K using the Kugelrohr apparatus. The obtained products were stored in a glovebox under an oxygen and water free (<1 ppm) nitrogen atmosphere

previously to the FT-ICR-MS experiments. The absence of residual solvent in all alkali metal samples was confirmed by DSC and thermogravimetric analysis (see below).

Li(NTf$_2$). Elemental analysis for $C_2NO_4S_2F_6Li$: expected C 8.37%, H 0.00%, N 4.88%; found C 8.90%, H 0.34%, N 4.83%. The onset (T_{on}) and maximum (T_{max}) temperatures of the fusion peak obtained by DSC were $T_{on} = 509.5 \pm 0.9$ K and $T_{max} = 512.7 \pm 0.5$ K, respectively and the corresponding specific enthalpy of fusion $\Delta_{fus}h = 45.84 \pm 1.84$ J·g^{-1}. The uncertainties quoted are twice the standard deviation of the mean of three determinations. Only the thermal decomposition of the compound with onset at $T_{on} = 604$ K was observed in the range covered by the TG experiments.

Na(NTf$_2$). Elemental analysis for $C_2NO_4S_2F_6Na$: expected C 7.92%, H 0.00%, N 4.62%; found C 7.95%, H 0.00%, N 4.87%. DSC (fusion): $T_{on} = 533.0 \pm 0.3$ K and $T_{max} = 537.6 \pm 0.2$ K, and $\Delta_{fus}h = 126.63 \pm 4.03$ J·g^{-1}. TG (thermal decomposition): $T_{on} = 660$ K.

K(NTf$_2$). Elemental analysis for $C_2NO_4S_2F_6K$: expected C 7.52%, H 0.00%, N 4.39%; found C 7.54%, H 0.00%, N 4.50%. DSC (fusion): $T_{on} = 474.9 \pm 0.7$ K and $T_{max} = 478.9 \pm 0.5$ K, and $\Delta_{fus}h = 78.89 \pm 2.97$ J·g^{-1}. TG (thermal decomposition): $T_{on} = 666$ K.

Rb(NTf$_2$). Elemental analysis for $C_2NO_4S_2F_6Rb$: expected C 6.57%, H 0.00%, N 3.83%; found C 6.57%, H 0.00%, N 4.14%. DSC (fusion): $T_{on} = 452.5 \pm 1.0$ K and $T_{max} = 455.0 \pm 1.4$ K, and $\Delta_{fus}h = 56.47 \pm 3.40$ J·g^{-1}. TG (thermal decomposition): $T_{on} = 634$ K.

Cs(NTf$_2$). Elemental analysis for $C_2NO_4S_2F_6Cs$: expected C 5.82%, H 0.00%, N 3.39%; found C 5.83%, H 0.00%, N 4.02%. DSC (fusion): $T_{on} = 403.3 \pm 0.3$ K and $T_{max} = 407.1 \pm 0.2$ K, and $\Delta_{fus}h = 29.87 \pm 3.26$ J·g^{-1}. TG (thermal decomposition): $T_{on} = 632$ K.

The fusion temperatures (T_{on}) obtained in this work are systematically higher than those found in the literature: 506 ± 5 K[36] and 507 K[35] for Li(NTf$_2$); 530 ± 5 K[36] for Na(NTf$_2$); 472 ± 5 K[36] and 478 K[35] for K(NTf$_2$); 450 ± 5 K[36] for Rb(NTf$_2$); 395 ± 5 K[36] and 388 K[34] for Cs(NTf$_2$). In contrast, the thermal decomposition temperatures are considerably lower than those reported in a previous TG study:[36] 657 K for Li(NTf$_2$), 714 K for Na(NTf$_2$), 733 K for K(NTf$_2$), 740 K for Rb(NTf$_2$), and 745 K for Cs(NTf$_2$). Since the method of calculation of the published decomposition temperatures was not indicated, the observed large discrepancies relative to our data may simply result from the fact that they do not correspond to onsets (as in our case) but, for example, to inflection points in the mass loss measuring curves. Finally, the enthalpy of fusion of Li(NTf$_2$) indicated above is in good agreement with the value $\Delta_{fus}h = 46$ J·g^{-1}, which was also obtained by DSC.[35]

Fourier Transform Ion Cyclotron Resonance Mass Spectrometry. The FT-ICR-MS experiments were performed in a Finnigan FT/MS 2001-DT instrument, equipped with a 3 T superconducting magnet, and a Finnigan Venus Odyssey data system. The experimental procedure was previously described.[11] In brief, samples (~10 mg) of M(NTf$_2$) (M = Li, Na, K, Rb, Cs) or HNTf$_2$ were placed into small glass capillary tubes, which were mounted on the temperature-controlled tip of the probe arm of the FT-ICR mass spectrometer. The arm was inserted into the high vacuum chamber of the spectrometer, kept at 303 K and at a pressure of ~1.3×10^{-6} Pa, leaving the capillary opening positioned close to the FT-ICR cell. The temperature of the sample was gradually increased until positive ion and negative ion electron ionization mass spectra (70 eV) could be recorded. For all M(NTf$_2$) salts, this occurred above the fusion temperature of the compounds. Due to its comparatively much higher vapor pressure at ambient temperature, HNTf$_2$ was sublimed at 303 K. The FT-ICR mass spectra of the corresponding vapor phases were recorded as a function of temperature and electron-beam intensity. As in the case of the pure liquids, the mixture of the five M(NTf$_2$) molten salts was evaporated from a capillary mounted in the probe arm of the spectrometer, and several FT-ICR mass spectra of the corresponding vapor phase were recorded as a function of time at constant temperature.

The ion-neutral ion pair reactions were carried out with EI = 40 eV. The reactant ions were initially thermalized by collisions with argon at a pressure of ~1.3×10^{-4} Pa, or ~1.6×10^{-4} Pa in the case of HNTf$_2$. Argon was introduced in the instrument through a leak valve. Specific ions were selected and trapped in the FT-ICR cell under cyclotron movement for different periods of time before detection. The recording of a series of mass spectra at different delay times provided information about the reactivity of those ions with the neutral species present in the vapor originating from the distillation of the molten M(NTf$_2$) (M = Li, Na, K, Rb, or Cs) compounds, or sublimation of HNTf$_2$, and on the kinetic profile of the observed reactions. Ion isolation was performed using stored waveform inverse Fourier transform (SWIFT) excitation.[38] Neutral pressures were measured with a Bayard−Alpert-type ionization gauge.

Acknowledgment. This work was supported by Fundação para a Ciência e a Tecnologia, Portugal (Project PTDC/QUI/66199/2006). K.R.S. also wishes to thank the industrial members of QUILL, the ESF, and the EPSRC (Portfolio Partnership Scheme, grant no. EP/D029538/1) for support.

Supporting Information Available: Figures S1−S10 with the results of the DSC and TG analysis of the studied M(NTf$_2$) (M = Li, Na, K, Rb, Cs) salts. This material is available free of charge via the Internet at http://pubs.acs.org.

References and Notes

(1) Earle, M. J.; Esperança, J. M. S. S.; Gilea, M. A.; Canongia Lopes, J. N.; Rebelo, L. P. N.; Magee, J. W.; Seddon, K. R.; Widegren, J. A. *Nature* **2006**, *439*, 831–834.

(2) Øye, H.; Jagtoyen, M.; Oksefjell, T.; Wilkes, J. *Mater. Sci. Forum* **1991**, *73−75*, 183–190.

(3) Paulechka, Y. U.; Zaitsau, D. H.; Kabo, G. J.; Strechan, A. A. *Thermochim. Acta* **2005**, *439*, 158–160.

(4) Zaitsau, D. H.; Kabo, G. J.; Strechan, A. A.; Paulechka, Y. U.; Tschersich, A.; Verevkin, S. P.; Heintz, A. *J. Phys. Chem. A* **2006**, *110*, 7303–7306.

(5) Emel'yanenko, V. N.; Verevkin, S. P.; Heintz, A. *J. Am. Chem. Soc.* **2007**, *129*, 3930–3937.

(6) Armstrong, J. P.; Hurst, C.; Jones, R. G.; Licence, P.; Lovelock, K. R. J.; Satterley, C. J.; Villar-Garcia, I. J. *Phys. Chem. Chem. Phys.* **2007**, *9*, 982–990.

(7) Santos, L. M. N. B. F.; Canongia Lopes, J. N.; Coutinho, J. A. P.; Esperança, J. M. S. S.; Gomes, L. R.; Marrucho, I. M.; Rebelo, L. P. N. *J. Am. Chem. Soc.* **2007**, *129*, 284–285.

(8) Luo, H. M.; Baker, G. A.; Dai, S. *J. Phys. Chem. B* **2008**, *112*, 10077–10081.

(9) Stark, A.; Seddon, K. R. Ionic Liquids. In *Kirk-Othmer Encyclopedia of Chemical Technology*, 5th ed.; Seidel, A., Ed.; Wiley InterScience: New Jersey, Wienheim, 2007; Vol. 26, pp 836−920.

(10) Plechkova, N. V.; Seddon, K. R. *Chem. Soc. Rev.* **2008**, *37*, 123–150.

(11) Leal, J. P.; Esperança, J. M. S. S.; Minas da Piedade, M. E.; Canongia Lopes, J. N.; Rebelo, L. P. N.; Seddon, K. R. *J. Phys. Chem. A* **2007**, *111*, 6176–6182.

(12) Strasser, D.; Goulay, F.; Kelkar, M. S.; Maginn, E. J.; Leone, S. R. *J. Phys. Chem. A* **2007**, *111*, 3191–3195.

(13) Gross, J. H. *J. Am. Soc. Mass Spectrom.* **2008**, *19*, 1347–1352.

(14) Abdul-Sada, A. K.; Elaiwi, A. E.; Greenway, A. M.; Seddon, K. R. *Eur. J. Mass Spectrom.* **1997**, *3*, 245–247.

(15) Zabet-Moghaddam, M.; Krüger, R.; Heinzle, E.; Tholey, A. *J. Mass Spectrom.* **2004**, *39*, 1494–1505.
(16) Alfassi, Z. B.; Huie, R. E.; Milman, B. L.; Neta, P. *Anal. Bioanal. Chem.* **2003**, *377*, 159–164.
(17) Milman, B. L.; Alfassi, Z. B. *Eur. J. Mass Spectrom.* **2005**, *11*, 35–42.
(18) Dyson, P. J.; Khalaila, I.; Luettgen, S.; McIndoe, J. S.; Zhao, D. *Chem. Commun.* **2004**, 2204–2205.
(19) Gozzo, F. C.; Santos, L. S.; Augusti, R.; Consorti, C. S.; Dupont, J.; Eberlin, M. N. *Chem.—Eur. J.* **2004**, *10*, 6187–6193.
(20) Dorbritz, S.; Ruth, W.; Kragl, U. *Adv. Synth. Catal.* **2005**, *347*, 1273–1279.
(21) Henderson, M. A.; McIndoe, J. S. *Chem. Commun.* **2006**, 2872–2874.
(22) Chen, H.; Ouyang, Z.; Cooks, R. G. *Angew. Chem., Int. Ed.* **2006**, *45*, 3656–3660.
(23) Neto, B. A. S.; Santos, L. S.; Nachtigall, F. M.; Eberlin, M. N.; Dupont, J. *Angew. Chem., Int. Ed.* **2006**, *45*, 7251–7254.
(24) Yoshizawa, M.; Xu, W.; Angell, C. A. *J. Am. Chem. Soc.* **2003**, *125*, 15411–15419.
(25) Kreher, U. P.; Rosamilia, A. E.; Raston, C. L.; Scott, J. L.; Strauss, C. R. *Molecules* **2004**, *9*, 387–393.
(26) Treble, R. G.; Johnson, K. E.; Tosh, E. *Can. J. Chem.* **2006**, *84*, 915–924.
(27) Davidovits, P.; McFadden, D. L. *Alkali Halide Vapors: Structure Spectra and Reaction Dynamics*; Academic Press: New York, 1979.
(28) Sangster, J.; Pelton, A. D. *J. Phys. Chem. Ref. Data* **1987**, *16*, 509–561.
(29) Galwey, A. K. *J. Therm. Anal. Calorim.* **2005**, *82*, 23–40.
(30) Miller, R. C.; Kusch, P. *J. Chem. Phys.* **1956**, *25*, 860–876.
(31) Rudnyi, E. B.; Bonnell, D. M.; Hastie, I. M. *Vestn. Mosk. Univ., Ser. 2: Khim.* **1994**, *35*, 291–308.
(32) Watarai, A.; Kubota, K.; Yamagata, M.; Goto, T.; Nohira, T.; Hagiwara, R.; Ui, K.; Kumagai, N. *J. Power Sources* **2008**, *183*, 724–729.
(33) Kubota, K.; Nohira, T.; Goto, T.; Hagiwara, R. *J. Chem. Eng. Data* **2008**, *53*, 2144–2147.
(34) Foropoulos, J.; Desmarteau, D. D. *Inorg. Chem.* **1984**, *23*, 3720–3723.
(35) Lascaud, S.; Perrier, M.; Vallee, A.; Besner, S.; Prudhomme, J.; Armand, M. *Macromolecules* **1994**, *27*, 7469–7477.
(36) Hagiwara, R.; Tamaki, K.; Kubota, K.; Goto, T.; Nohira, T. *J. Chem. Eng. Data* **2008**, *53*, 355–358.
(37) Haas, A.; Klare, C.; Betz, P.; Bruckmann, J.; Kruger, C.; Tsay, Y. H.; Aubke, F. *Inorg. Chem.* **1996**, *35*, 1918–1925.
(38) Guan, S. H.; Marshall, A. G. *Int. J. Mass Spectrom.* **1996**, *158*, 5–37.

JP811039B